

Design of a Broadband Right-Angled Bend Using Transformation Optics

Mozhdeh Mola* and Alireza Yahaghi

Abstract—A right-angled waveguide bend using conformal transformation optics is proposed which guides the input electromagnetic wave smoothly through the waveguide, reduces the reflections and broadens the bandwidth of the device significantly. The isotropic material parameters are obtained through solving Laplace's equations with Dirichlet and Neumann boundary conditions. It is shown that the performance of the proposed bend is mainly determined by refractive indices lower than one. Utilizing this, the approximated resulting medium is implemented by drilling hole arrays in a dielectric background. In order to take advantage of planar technology, it can be implemented in a substrate integrated waveguide.

1. INTRODUCTION

Transformation optics (TO) has attracted remarkable attention in many fields, including physics, mathematics and many branches of engineering. TO is a powerful tool for creating novel electromagnetic (EM) and optical devices with a variety of unconventional properties. The fact that mapping on the metric of space can be translated into a change on constitutive parameters was considered almost a century ago [1, 2]. For example, coordinate transformation was frequently employed in design of perfectly matched layers (PML) in various coordinate systems [3, 4]. Some of TO's applications in computational EM are addressed in [5, 6]. TO was applied to design a cloaking device for the first time in 2006 [7, 8]. While cloaking is transforming an object to a point, the concept of transforming a certain PEC object to another shape, and extending the idea of cloaking to reshaping objects in EM scattering was first introduced by [9, 10]. TO is a technique to control and manipulate EM fields with a high degree of flexibility. In this method, a coordinate transformation corresponds to an inhomogeneous and anisotropic medium. This material interpretation is derived from the fact that the form of Maxwell's equations are invariant under coordinate transformation with altered coefficients for material parameters. This means that the desired field distribution is designed in a virtual curved coordinate and it is acquired in a flat Cartesian coordinate, filled by a proper transformation medium whose material parameters are completely specified by the transformation definition. Even though TO is mainly well known for cloaking, it has several applications other than invisibility. Since 2006, a large number of innovative EM devices have been proposed; including field rotators [11–13], concentrators [14–16], splitters [12], beam bends [17–24], antennas [25, 26] and imaging systems [27–29], but few of them are experimentally realized due to the requirement of implementing simultaneously anisotropic and inhomogeneous electric permittivity and magnetic permeability resulted from traditional TO. Although metamaterials have the capability of exhibiting a wide range of permittivity and permeability, including extreme values, they often suffer from a resonant response which leads to an extremely narrow band and unavoidable losses [30].

Received 15 December 2014, Accepted 16 March 2015, Scheduled 1 April 2015

* Corresponding author: Mozhdeh Mola (mozhdeh.mola@gmail.com).

The authors are with the School of Electrical and Computer Engineering, College of Engineering, Shiraz University, Shiraz, Iran.

Many efforts have been made to simplify these material parameters [31,32]. There are some major approaches for yielding simple constitutive parameters. The first and most straightforward method is to make approximation to the obtained design to achieve material simplicity [31]; the second method is to apply numerical optimization techniques that begins with transformation design, to find realizable material parameters [33]. The third procedure uses the degrees of freedom associated with the transformation itself which is applied in this paper.

Since there are a large number of transformations that exhibit same functionality, one can choose an appropriate transformation that minimizes the anisotropy. A numerical technique based on quasi-conformal mapping was first introduced by Pendry and Li [32] which results in an approximately isotropic carpet cloak with a broadband behaviour. Besides, strict conformal mapping gives rise to ability of steering EM field in a pre-determined way using isotropic material [34]. After establishment of these methods as subsets of general TO, many new quasi-conformal and strict conformal transformation based devices have been proposed [35–38].

Waveguide bends are important components which are used to change direction of propagation and to interconnect straight waveguides and input/output ports. They have also applications in multiplexers [39], microwave filters [40], radar seekers and satellite communication systems [41]. Waveguides are the most efficient way to transfer EM energy with minimum radiation losses, but any abrupt changes in their size or shape such as bending, excites higher order modes, which restrict the bandwidth. To overcome this difficulty, waveguide bends with long radius of curvature can be used. However, due to space limitations, compact waveguide bends are desired. There are some other common methods for improving waveguide bends' performance like putting metallic post [42], rounding the outer corner or chamfering it [43], but all these methods are narrow band and can improve the transmission characteristics only in the single-mode operation's bandwidth. Therefore, designing a compact waveguide bend with low reflections and broad bandwidth is of great importance.

Extending TO to the design of waveguides and utilizing anisotropic metamaterial layers based on coordinate transformation for improving waveguide characteristics [44] and in particular for reflectionless waveguide bends [45] were first introduced in 2007 and 2008, respectively. TO can contribute to a novel perspective on wave guiding and upgrading traditional waveguides. There are three kinds of TO waveguide bends based on different mappings. First, *non-conformal mapping* [46] which is the most general one and normally leads to inhomogeneous, anisotropic and magnetic materials. Although metamaterials provide a wide range of material parameters, they usually have usually resonant characteristics which result in narrow band and lossy response. As a result, because of implementation difficulties, the obtained bend is approximated to a nonmagnetic material [47] or homogeneous and isotropic material but with negative refractive index [48] or some alternating layers of anisotropic materials [49]. These approximations generally degrade the performance of the designed bend. The second one is *conformal mapping* [50] that provides the design with isotropic materials. The last one is *quasi-conformal mapping* [32] which is a compromise between two above mentioned methods. It minimizes the anisotropy of the original material parameters to yield approximately isotropic material.

Furthermore, recently, substrate integrated waveguide (SIW) technology has been proposed with low radiation losses, high quality factor and high power capacity. It consists of periodic arrays of metallic posts embedded in a substrate with metallic shields on the top and bottom to mimic the walls of a rectangular waveguide. It has the advantages of both traditional rectangular waveguides and microstrips. This structure has a smaller size than rectangular waveguides and can be simply realized on a printed circuit board with low cost fabrication techniques [51].

In this paper, by taking advantage of strict conformal transformation and SIW technology, an implementation procedure for realizing a broadband right-angled waveguide bend with negligible reflection is proposed. The challenging part is to realize the inhomogeneous isotropic material with relatively large range of refractive indices. Based on effective medium theory, the designed waveguide bend can be realized by drilling hole arrays in the substrate.

2. DESIGN OF A BROADBAND RIGHT-ANGLED WAVEGUIDE BEND

A two-dimensional conformal transformation has been proposed to design a reflectionless bend for TE polarization in [36]. To determine the required conformal transformation, a straightforward numerical

technique has been proposed, which is performed by solving two Laplace's equations. According to Riemann mapping theorem, any quadrilateral can be mapped to a rectangle with the same conformal module. The conformal module for a rectangle is defined by its length to width ratio. As it is explained in [36], to avoid mixed boundary conditions, the inverse conformal transformation is derived by solving following Laplace's equation with classical boundary conditions (Dirichlet's and Neumann's boundary condition) applied on physical domain:

$$\eta|_{\Gamma_1} = 0, \quad \eta|_{\Gamma_3} = a \quad \text{and} \quad \vec{n} \cdot \nabla \eta|_{\Gamma_1, \Gamma_3} = 0 \tag{1}$$

for function $\eta(x, y)$ and

$$\xi|_{\Gamma_1} = 0, \quad \xi|_{\Gamma_3} = aM \quad \text{and} \quad \vec{n} \cdot \nabla \xi|_{\Gamma_2, \Gamma_4} = 0 \tag{2}$$

for function $\xi(x, y)$, where (η, ξ) denotes the virtual Cartesian coordinate system, (x, y) the physical Cartesian coordinate system (Figure 1), M the ratio of two sides of the rectangle in virtual domain which is calculated by $M = 1/a \int_{\Gamma_4} |\partial\eta/\partial n| ds$, $a = \Gamma'_1$ a scaling factor (Figure 1), and \vec{n} the outpointing normal vector to the boundaries.

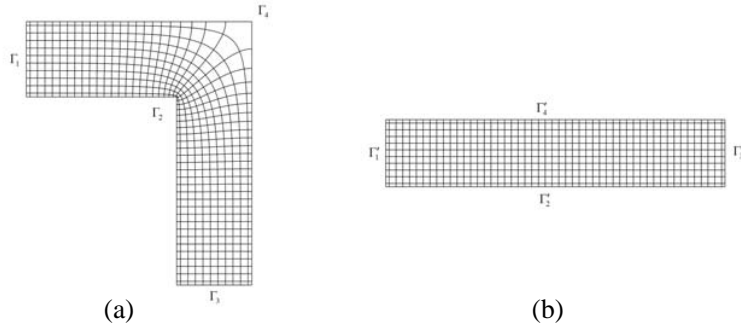


Figure 1. (a) Physical domain. (b) Virtual domain.

Finally, the constitutive parameters of the physical space are calculated by:

$$\epsilon = \frac{\epsilon_r}{\det \Lambda'^{-1}} = [(\xi_x)^2 + (\eta_x)^2] \epsilon_r, \quad \mu = 1 \tag{3}$$

where Λ' is the obtained inverse transformation matrix; $\xi(x, y)$ and $\eta(x, y)$ are the coordinates in the virtual domain; ξ_x and η_x are their derivatives with respect to x . Through this procedure, the Laplace's equations are solved using COMSOL Multiphysics [52].

3. IMPLEMENTATION OF REFRACTIVE INDEX BY DRILLING HOLE ARRAYS

As can be seen in Eq. (3), the material parameters are isotropic but inhomogeneous; hence, they can be realized by dielectric materials. Utilizing the method described above, the electric permittivity of the waveguide bend ranges from about zero to 24. The electric permittivity distribution depends on the bend's dimension, scaling factor a and ϵ_r in Eq. (3) which is chosen to be one here. Moreover, the scaling factor a is chosen so as to yield refractive index equal to one near input and output ports. As it can be seen in Figure 2(a), the highest values lie around the internal corner while the lowest ones are around the external corner. With this index profile, and assuming the boundaries to be PEC, the input wave is guided through the waveguide smoothly and the scattering parameter S_{21} (Figure 2(c)) shows that the wave is completely transmitted in the whole frequency band. In fact the corresponding phase velocity difference between the refractive indices in internal and external corners will guide the wave around the bend.

In order to implement this profile using dielectric materials, refractive indices lower than one have to be replaced by unity. To see how this approximation affects the bend's performance, the waveguide with this nondispersive refractive index profile is simulated (Figure 3).

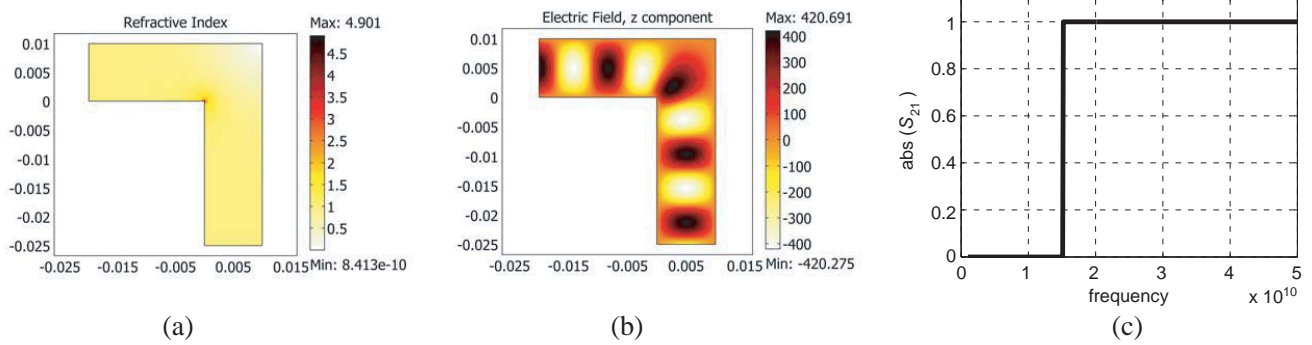


Figure 2. (a) Refractive index profile of an ideal bend obtained by conformal transformation. The width w of waveguide is 0.01 m. (b) z component of electric field at 30 GHz (about twice the cut-off frequency). (c) S_{21} parameter of the bend.

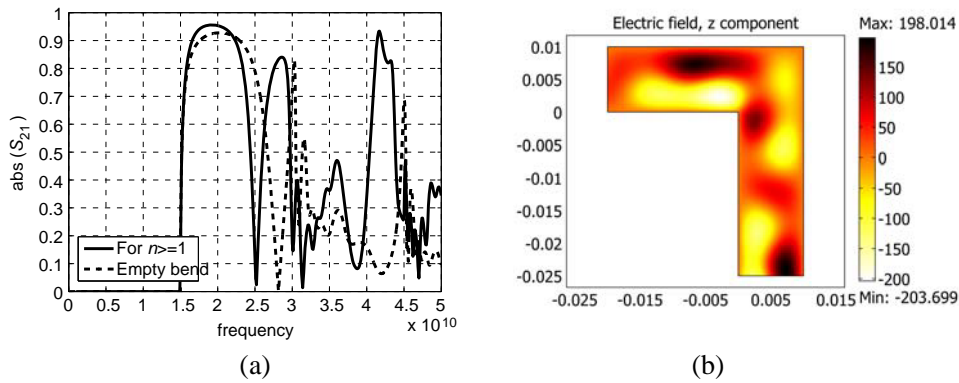


Figure 3. (a) S_{21} parameter of the bend (the refractive indices lower than one have been excluded). (b) z component of electric field at 30 GHz (about twice the cut-off frequency).

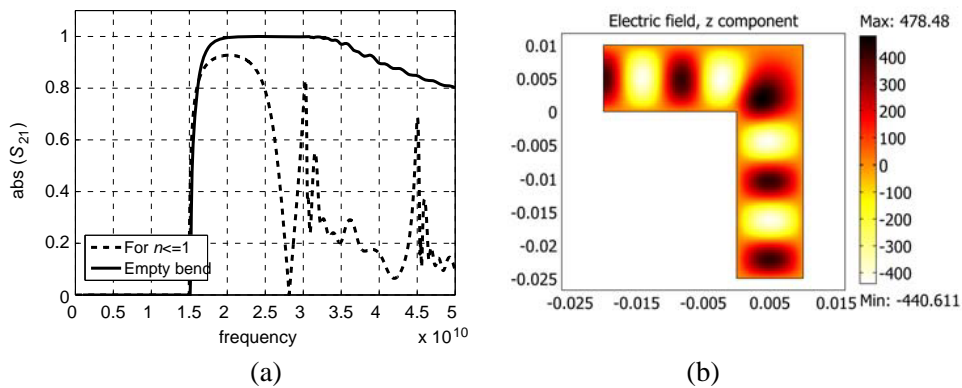


Figure 4. (a) S_{21} parameter of the bend (the refractive indices higher than one have been excluded). (b) z component of electric field at 30 GHz (twice the cut-off frequency).

It can be recognized that a considerable performance degradation is resulted comparing to the ideal design. It is concluded that the refractive indices higher than one have a negligible impact on the operation. Accordingly, the case of refractive indices lower than one is simulated (Figure 4).

The results show that refractive indices lower than one have the main influence on the bend's

functionality and increase the bandwidth extensively comparing to an empty bend with the same dimensions. As it is seen from Figure 4, the reflection is negligible almost in the whole frequency band and the field transmission is higher than 0.8.

To implement the refractive index profile of this case — with electric permittivities lower than one — resonant metamaterials including metallic structures are required. These metamaterials usually suffer from narrow bandwidths and unavoidable losses. To prevent these complex composites, the ϵ_r in Eq. (3) can be chosen to be a relatively large number. Consequently, the profile will be multiplied by a large ϵ_r and a part of the relative permittivities will exceed unity. Neglecting remaining dispersive values, the resulting refractive index distribution can be approximated to introducing array of air holes with spatially varying radii in a background dielectric. The substrate chosen here is TMM13i [53] with $\epsilon_d = 12.2$. Therefore, relative permittivities between 1 and 12.2 can be realized through drilling holes into this substrate. Different ϵ_r in Eq. (3) can be opted for reaching this range. In fact, an interval $[1/\epsilon_r, 12.2/\epsilon_r]$ of original profile is chosen and multiplied by ϵ_r to achieve the desired implementable range for refractive indices. As discussed above, by choosing ϵ_r equal to one or less the bandwidth won't increase (Figure 3). It can be shown that the optimum value of ϵ_r is around 5, as it increases, the performance will deteriorate and for values larger than 14 the operation isn't better than a simple right-angled bend.

In [54], a method based on effective medium theory has been described to specify the radii of air holes or electric rods for implementing a gradient-index profile. In this strategy, a smoothly varying continuous refractive index is first estimated to a discrete form with square cells of side d , and the cell refractive index n_{ij} associated with ij -cell. Next, radii of holes or rods can be determined for TE polarization by:

$$r_{ij} = d \sqrt{\frac{n_{ij}^2 - \epsilon_{host}}{\pi(\epsilon_{rod} - \epsilon_{host})}} \quad (4)$$

where ϵ_{host} refers to the electric permittivity of the background dielectric, and ϵ_{rod} refers to that of the rods.

By further exploration of the original refractive index profile (Figure 2(a)) it is revealed that much of the bend's area has refractive indices about 1, so when it is multiplied by $\sqrt{\epsilon_r}$. The refractive index near input and output ports will change and affect the cut-off frequency. Besides, since we are using TMM13i with $\epsilon_d = 12.2$, for putting the resulting profile into practice, it is necessary to drill the whole area of the bend for all values of ϵ_r except 12.2. Moreover, to prevent the holes from intersecting, the ratio of $2r_{ij}/d$ should be smaller than one. According to Eq. (4), n_{ij} must be larger than 1.846 for our substrate to fulfil this criterion. Because of this extra limitation, refractive indices less than 1.846 should be replaced by 1.846. This can be a considerable part of the bend's area especially for smaller values of ϵ_r , and thus will deteriorate its performance dramatically. It is concluded that $\epsilon_r = \epsilon_d = 12.2$ will be the best option especially for fabrication ease.

After multiplying original dielectric constant profile by $\epsilon_r = 12.2$ all the values lower than one are replaced by one and those which are greater than 12.2 are replaced by 12.2. The simulated results of the proposed structure is shown in Figure 5. Around the external corner, there exist a domain that its refractive indices have been replaced by unity and consequently for its implementation, the whole substrate should be removed. Although it will change the PEC boundaries, it is quite beneficial from the fabrication point of view to chamfer the external corner of the bend (Figure 6(b)), besides the performance will not be affected too much (Figure 6(a)).

It can be seen from Figure 6 that the holes with different radii have effectively simulated the desired refractive index distribution. Larger unit cells lead to a more simplified realization procedure. Therefore, a compromise should be made between ease of fabrication and acceptable performance. Results for simulation of a bend with smaller number of holes are depicted in Figure 7.

Figure 7 shows that increasing the cells' side will reduce the bend's performance but leads to a simpler fabrication.

An alternative way of employing Eq. (4) is to implement the refractive index profile by varying d (cells' side) while r_{ij} (hole radius) is kept constant for all holes. To simplify the approach, the domain, in which the holes have to be drilled, is divided into four regions, and an average refractive index is considered for each region. Having a fixed refractive index and a fixed radius, the cells' side d in each

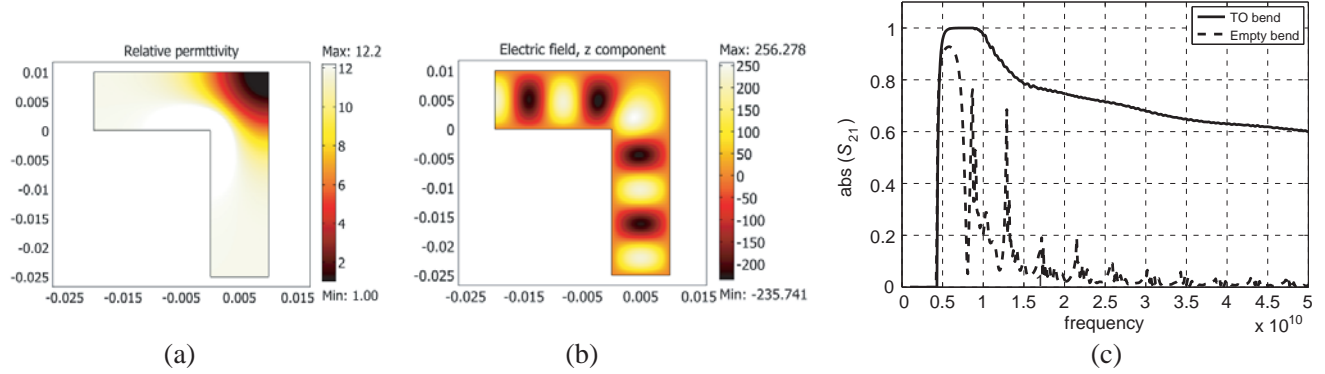


Figure 5. (a) Refractive indices between 1 and 12.2. (b) z component of electric field at 8.6 GHz (about twice the cut-off frequency). (c) S_{21} parameter of the bend.

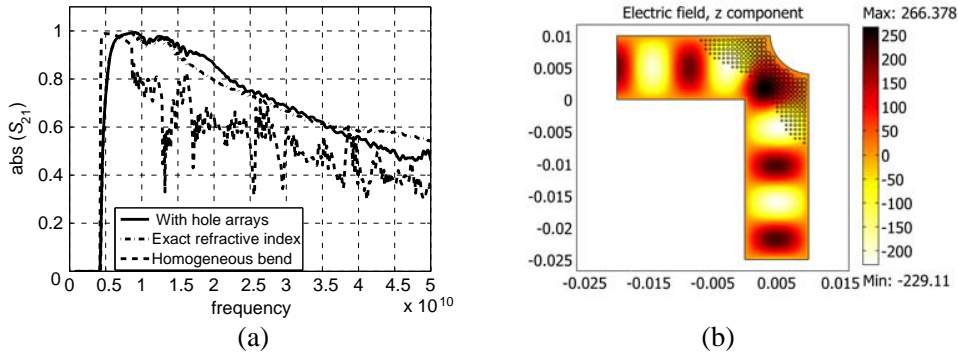


Figure 6. (a) S_{21} parameter of the bend with drilled holes (constant cells' side $d = 0.7$ mm but different radii). (b) z component of electric field at 8.6 GHz (about twice the cut-off frequency).

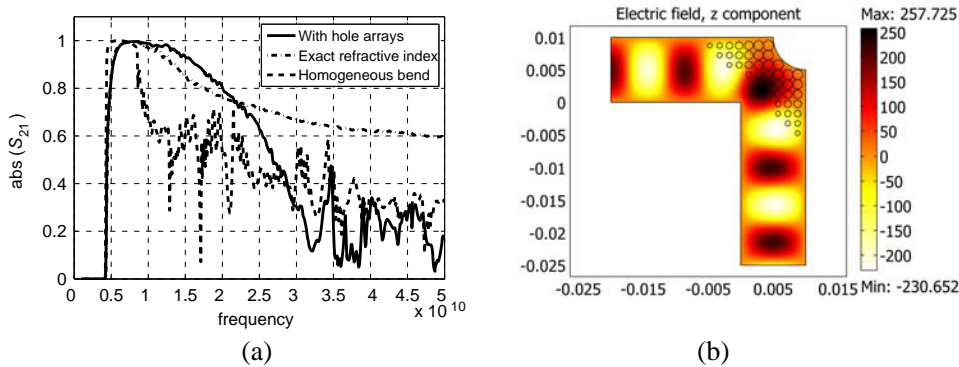


Figure 7. (a) S_{21} parameter of the bend with hole arrays (cells' side $d = 1.5$ mm in Eq. (4)). (b) z component of electric field at 8.6 GHz.

region is obtained using Eq. (4) (Figure 8).

For taking advantage of the proposed procedure in planar structures technology, the obtained structure can be realized by SIW. The designing parameters of SIW such as radius r_s of posts and spacing between two adjacent posts w_s can be determined based on equivalence of traditional rectangular waveguide and SIW [55]. These parameters are chosen such that the width and consequently the cut-off

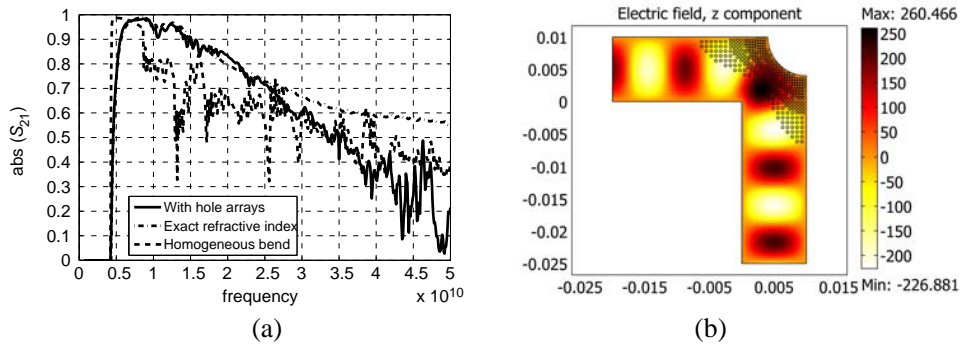


Figure 8. (a) S_{21} parameter of the bend with hole arrays of constant radii equal to 0.2 mm. (b) z component of electric field at 8.6 GHz.

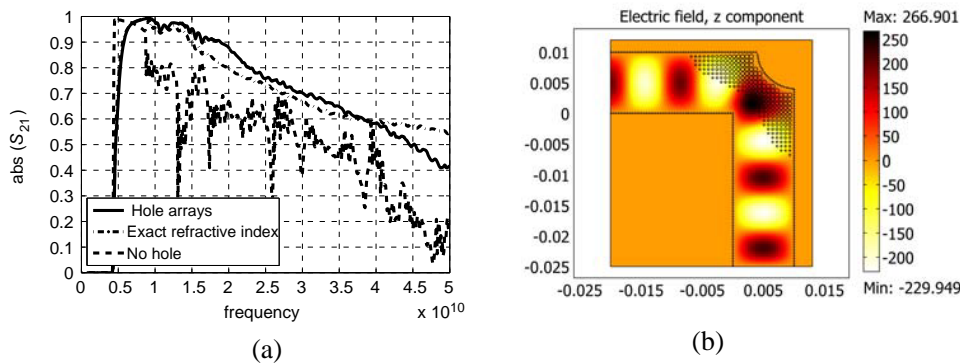


Figure 9. (a) S_{21} parameter of the SIW bend with drilled holes (constant cells' side $d = 0.7$ mm and different radii). (b) z component of electric field at 8.6 GHz

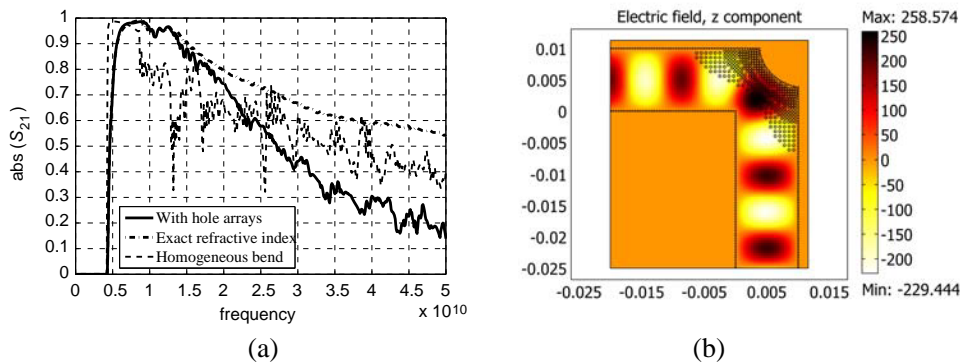


Figure 10. (a) S_{21} parameter of the SIW bend with drilled holes (constant radii is set to 0.2 mm). (b) z component of electric field at 8.6 GHz.

frequency of both SIW and its equivalent rectangular waveguide are the same. The equivalent SIW bend of the proposed waveguide bends in Figures 6 and 8 are simulated, and their results are shown in Figures 9 and 10, respectively.

It is seen from Figures 9 and 10 that there is a good agreement between these SIW bend structures and previous equivalent rectangular waveguides.

4. THREE DIMENSIONAL SIMULATION

To validate the idea for a real 3D rectangular waveguide bend with improved characteristics, the bend in Figure 7 is simulated as a three-dimensional rectangular waveguide using HFSS [56]. Figure 11(a) shows this 3D structure which is proposed as a realizable model with a moderate number of holes (43 holes) and relatively large holes' radius. Its S_{21} parameter is compared to that of a similar homogeneous rectangular waveguide bend. It is seen from Figure 11(c) that the bandwidth becomes twice wider by drilling these holes in the dielectric ($\epsilon_d = 12.2$) inside the waveguide bend. In Figure 11(b) magnitude of electric field in the waveguide is depicted at 10 GHz.

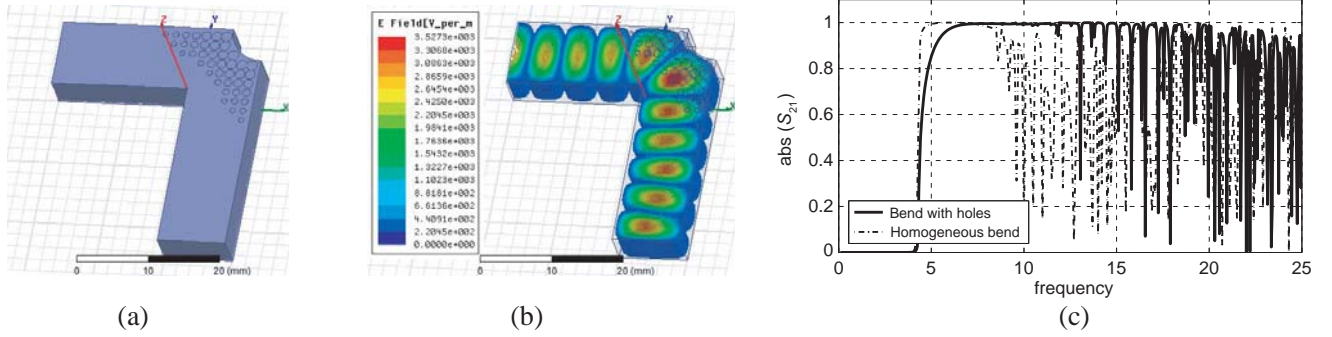


Figure 11. (a) 3D structure of rectangular waveguide bend with hole arrays (cells' side $d = 1.5$ mm and dielectric constant $\epsilon_d = 12.2$), the width w and the height h of the waveguide are 0.01 m and 0.00508 m respectively. (b) Magnitude of electric field at 10 GHz. (c) S_{21} parameter of the obtained waveguide bend comparing to that of a similar homogeneous waveguide bend.

At the end, a designing procedure for any other bends with arbitrary size and bandwidth of operation can be organized as below:

1. Solving two Laplace's equations and yielding corresponding permittivity profile.
2. Adjusting scaling factor a in Eqs. (1) and (2) so as to have permittivity equal to one near input and output ports (resulting refractive indices and scaling factor a have linear relationship).
3. Choosing a substrate with dielectric constant equal to ϵ_d as the dielectric background.
4. Assuming an interval $[1/\epsilon_r, \epsilon_d/\epsilon_r]$ from original permittivity distribution.
5. Choosing a proper ϵ_r according to fabrication consideration and desired cut-off frequency and bandwidth. The cut-off frequency is obtained by $f_{c0} = \frac{c}{2w\sqrt{\epsilon_r}}$ where c is light velocity in vacuum, w is the width of waveguide and ϵ_r is the permittivity near ports.
6. Multiplying permittivity profile by ϵ_r and confining the range within $[1, \epsilon_d]$ interval by replacing lower than one permittivities by one and higher than ϵ_d by ϵ_d .
7. Applying Eq. (4) to calculate radii for drilling holes.

5. CONCLUSION

An implementation procedure is proposed for a broadband right-angled bend obtained from conformal transformation optics. It is shown that the main functionality depends on refractive indices lower than one. They are multiplied by a relatively large number to avoid dispersive metamaterials, and the profile is approximated by hole arrays in a background dielectric. The simulation results show that the acquired structures are not very sensitive to approximations made to derive material parameters. The designed waveguide can be realized by SIW technology which is compatible with planar circuits. All these features lead to a simple and efficient implementation. At the end, the idea is validated by simulation of a real 3D waveguide bend.

REFERENCES

1. Bateman, H., "The transformation of the electro-dynamical equations," *Proc. London Math. Soc.*, Vol. 8, 223–264, 1910.
2. Van Dantzig, D., "The fundamental equations of electromagnetism, independent of metrical geometry," *Proc. Cambridge Phil. Soc.*, Vol. 30, 421–427, 1934.
3. Teixeira, F. L. and W. C. Chew, "Analytical derivation of a conformal perfectly matched absorber for electromagnetic waves," *Microwave Opt. Technol. Lett.*, Vol. 17, No. 4, 231–236, 1998.
4. Teixeira, F. L. and W. C. Chew, "Differential forms, metrics, and the reflectionless absorption of electromagnetic waves," *Journal of Electromagnetic Waves and Applications*, Vol. 13, No. 5, 665–686, 1999.
5. Ward, A. J. and J. B. Pendry, "Refraction and geometry in Maxwell's equations," *J. Mod. Opt.*, Vol. 43, No. 4, 773–793, 1996.
6. Teixeira, F. L. and W. C. Chew, "Lattice electromagnetic theory from a topological viewpoint," *J. Math. Phys.*, Vol. 40, No. 1, 169–187, 1999.
7. Leonhardt, U., "Optical conformal mapping," *Science*, Vol. 312, 1777–1780, 2006.
8. Pendry, J. B., D. Schurig, and D. R. Smith, "Controlling electromagnetic fields," *Science*, Vol. 312, 1780–1782, 2006.
9. Teixeira, F. L., "Closed-form metamaterial blueprints for electromagnetic masking of arbitrarily shaped convex PEC objects," *IEEE Antennas Wireless Propagat. Lett.*, Vol. 6, 163–164, 2007.
10. Ozgun, O. and M. Kuzuoglu, "Electromagnetic metamorphosis: Reshaping scatterers via conformal anisotropic metamaterial coatings," *Microwave Opt. Technol. Lett.*, Vol. 49, No. 10, 2386–2392, 2007.
11. Chen, H., B. Hou, S. Chen, X. Ao, W. Wen, and C. Chan, "Design and experimental realization of a broadband transformation media field rotator at microwave frequencies," *Physical Review Letters*, Vol. 102, 183903, 2009.
12. Kwon, D.-H. and D. H. Werner, "Polarization splitter and polarization rotator designs based on transformation optics," *Optics Express*, Vol. 16, 18731–18738, 2008.
13. Luo, Y., H. Chen, J. Zhang, L. Ran, and J. A. Kong, "Design and analytical full-wave validation of the invisibility cloaks, concentrators, and field rotators created with a general class of transformations," *Physical Review B*, Vol. 77, 125127, 2008.
14. Jiang, W. X., T. J. Cui, Q. Cheng, J. Y. Chin, X. M. Yang, R. Liu, and D. R. Smith, "Design of arbitrarily shaped concentrators based on conformally optical transformation of nonuniform rational B-spline surfaces," *Applied Physics Letters*, Vol. 92, 264101-1–264101-3, 2008.
15. Rahm, M., D. Schurig, D. A. Roberts, S. A. Cummer, D. R. Smith, and J. B. Pendry, "Design of electromagnetic cloaks and concentrators using form-invariant coordinate transformations of Maxwell's equations," *Photonics and Nanostructures-Fundamentals and Applications*, Vol. 6, 87–95, 2008.
16. Wang, W., L. Lin, J. Ma, C. Wang, J. Cui, C. Du, and X. Luo, "Electromagnetic concentrators with reduced material parameters based on coordinate transformation," *Optics Express*, Vol. 16, 11431–11437, 2008.
17. Ding, W., D. Tang, Y. Liu, L. Chen, and X. Sun, "Arbitrary waveguide bends using isotropic and homogeneous metamaterial," *Applied Physics Letters*, Vol. 96, 041102-1–041102-3, 2010.
18. Han, T., C.-W. Qiu, J.-W. Dong, X. Tang, and S. Zouhdi, "Homogeneous and isotropic bends to tunnel waves through multiple different/equal waveguides along arbitrary directions," *Optics Express*, Vol. 19, 13020–13030, 2011.
19. Jiang, W. X., T. J. Cui, X. Y. Zhou, X. M. Yang, and Q. Cheng, "Arbitrary bending of electromagnetic waves using realizable inhomogeneous and anisotropic materials," *Physical Review E*, Vol. 78, 066607, 2009.
20. Mei, Z. L. and T. J. Cui, "Arbitrary bending of electromagnetic waves using isotropic materials," *Journal of Applied Physics*, Vol. 105, 104913-1–104913-5, 2009.

21. Rahm, M., D. Roberts, J. Pendry, and D. Smith, "Transformation-optical design of adaptive beam bends and beam expanders," *Optics Express*, Vol. 16, 11555–11567, 2008.
22. Roberts, D., M. Rahm, J. Pendry, and D. Smith, "Transformation-optical design of sharp waveguide bends and corners," *Applied Physics Letters*, Vol. 93, 251111-1–251111-3, 2008.
23. Wu, X., Z. Lin, H. Chen, and C. Chan, "Transformation optical design of a bending waveguide by use of isotropic materials," *Applied Optics*, Vol. 48, G101–G105, 2009.
24. Xu, H., B. Zhang, T. Yu, G. Barbastathis, and H. Sun, "Dielectric waveguide bending adapter with ideal transmission: Practical design strategy of area-preserving affine transformation optics," *JOSA B*, Vol. 29, 1287–1290, 2012.
25. Aghanejad, I., H. Abiri, and A. Yahaghi, "Design of high-gain lens antenna by gradient-index metamaterials using transformation optics," *IEEE Trans. Antennas Propag.*, Vol. 60, No. 9, 4074–4081, 2012.
26. Luo, Y., J. Zhang, H. Chen, J. Huangfu, and L. Ran, "High-directivity antenna with small antenna aperture," *Applied Physics Letters*, Vol. 95, 193506, 2009.
27. Yan, M., W. Yan, and M. Qiu, "Cylindrical superlens by a coordinate transformation," *Physical Review B*, Vol. 78, 125113, 2008.
28. Smith, D. R., Y. Urzhumov, N. B. Kundtz, and N. I. Landy, "Enhancing imaging systems using transformation optics," *Optics Express*, Vol. 18, 21238–21251, 2010.
29. Roberts, D., N. Kundtz, and D. Smith, "Optical lens compression via transformation optics," *Optics Express*, Vol. 17, 16535–16542, 2009.
30. Gney, D., T. Koschny, and C. M. Soukoulis, "Reducing ohmic losses in metamaterials by geometric tailoring," *Physical Review B*, Vol. 80, 125129, 2009.
31. Schurig, D., J. Mock, B. Justice, S. Cummer, J. Pendry, A. Starr, and D. R. Smith, "Metamaterial electromagnetic cloak at microwave frequencies," *Science*, Vol. 314, 977–980, 2006.
32. Li, J. and J. Pendry, "Hiding under the carpet: A new strategy for cloaking," *Physics Optics*, arXiv Preprint arXiv: 0806.4396, 2008.
33. Popa, B.-I. and S. A. Cummer, "Cloaking with optimized homogeneous anisotropic layers," *Physical Review A*, Vol. 79, 023806, 2009.
34. Turpin, J. P., A. T. Massoud, Z. H. Jiang, P. L. Werner, and D. H. Werner, "Conformal mappings to achieve simple material parameters for transformation optics devices," *Optics Express*, Vol. 18, 244–252, 2010.
35. Landy, N. I. and W. J. Padilla, "Guiding light with conformal transformations," *Optics Express*, Vol. 17, No. 1, 14879–4872, 2009.
36. Ma, Y., N. Wang, and C. Ong, "Application of inverse, strict conformal transformation to design waveguide devices," *JOSA A*, Vol. 27, 968–972, 2010.
37. Mei, Z.-L., J. Bai, T. M. Niu, and T.-J. Cui, "A planar focusing antenna design with the quasi-conformal mapping," *Progress In Electromagnetics Research M*, Vol. 13, 261–273, 2010.
38. Garcia-Meca, C., A. Martinez, and U. Leonhardt, "Engineering antenna radiation patterns via quasi-conformal mappings," *Optics Express*, Vol. 19, 23743–23750, 2011.
39. Liang, X.-P., K. A. Zaki, and A. E. Atia, "A rigorous three plane mode-matching technique for characterizing waveguide T-junctions and its application in multiplexer design," *IEEE Trans. Microwave Theory and Techniques*, Vol. 39, No. 12, 2138–2147, Dec. 1991.
40. Liang, X.-P., "Modeling of dual mode dielectric resonator filters and multiplexers," Ph.D. Dissertation, University of Maryland at College Park, 1993.
41. Peverini, O., G. Virone, R. Tascone, and G. Addamo, "Passive microwave feed chains for high-capacity satellite communications systems," *Advances in Satellite Communications*, Dr. M. Karimi, Ed., InTech, 2011, ISBN: 978-953-307-562-4.
42. Djerafi, T. and K. Wu, "Super-compact substrate integrated waveguide cruciform directional coupler," *IEEE Microwave and Wireless Components Letters*, Vol. 17, No. 11, 757–759, 2007.
43. Bochra R., et al., "Design of optimal chamfered bends in rectangular substrate integrated waveguide," *IJCSI International Journal of Computer Science Issues*, Vol. 8, Issue 4, No. 2, 376–

- 379, Jul. 2011.
44. Ozgun O. and M. Kuzuoglu, "Utilization of anisotropic metamaterial layers in waveguide miniaturization and transitions," *IEEE Microwave and Wireless Components Letters*, Vol. 17, No. 11, 754–756, 2007.
 45. Donderici, B. and F. L. Teixeira, "Metamaterial blueprint for reflectionless waveguide bends," *IEEE Microwave and Wireless Components Letters*, Vol. 18, No. 4, 233–235, 2008.
 46. Pendry, J. B., D. Schurig, and D. R. Smith, "Controlling electromagnetic fields," *Science*, Vol. 312, 1780–1782, 2006.
 47. Xu, H., B. Zhang, T. Yu, et al., "Dielectric waveguide bending adapter with ideal transmission: Practical design strategy of area-preserving affine transformation optics," *J. Opt. Soc. Am. B*, Vol. 29, 1287–1290, 2012.
 48. Ding, W., D. Tang, Y. Liu, L. Chen, and X. Sun, "Arbitrary waveguide bends using isotropic and homogeneous metamaterial," *Applied Physics Letters*, Vol. 96, 041102-1–041102-3, 2010.
 49. Wu, X., Z. Lin, H. Chen, and C. Chan, "Transformation optical design of a bending waveguide by use of isotropic materials," *Applied Optics*, Vol. 48, G101–G105, 2009.
 50. Heiblum, M. and J. Harris, "Analysis of curved optical waveguides by conformal transformation," *IEEE J. Quantum. Electron.*, Vol. 11, 75–83, 1975.
 51. Wu, X. H. and A. A. Kishk, "Analysis and design of substrate integrated waveguide using efficient 2D hybrid method," *Synthesis Lectures on Computational Electromagnetics*, Vol. 5, 1–90, 2010.
 52. <https://www.comsol.com/>.
 53. <http://www.rogerscorp.com/acm/products/51/TMM-13i-Laminates.aspx>.
 54. Vasic, B., G. Isic, R. Gajic, and K. Hingerl, "Controlling electromagnetic fields with graded photonic crystals in metamaterial regime," *Optics Express*, Vol. 18, 20321–20333, 2010.
 55. Che, W., K. Deng, D. Wang, and Y. Chow, "Analytical equivalence between substrate-integrated waveguide and rectangular waveguide," *IET Microwaves, Antennas and Propagation*, Vol. 2, 35–41, 2008.
 56. <http://www.ansys.com/>.